Influence of binary evolution on properties of red supergiants

Bachelorarbeit in Physik von

Ariana Aglaia Leu

angefertigt im Argelander-Institut für Astronomie

vorgelegt der Mathematisch-Naturwissenschaftlichen Fakultät der Universität Bonn

Februar 2019

Ich versichere, dass ich diese Arbeit selbständig verfasst und keine anderen als die angegebenen Quellen und Hilfsmittel benutzt sowie die Zitate kenntlich gemacht habe.

Bonn, den..... Unterschrift.....

1. Gutachter(in): Prof. Dr. Norbert Langer
2. Gutachter(in): Dr. Jürgen Kerp

Contents

Chapter 1

Introduction

1.1 Stellar clusters and red stragglers

We refer to a stellar cluster as an accumulation of stars, that can be gravitationally bound but is not necessarily. All stars in the cluster are expected to have formed at the same time and to therefore have the same age. Observations of stellar clusters, however, discovered some massive stars that seem to have a much younger age than the other stars, so that the age of stars in the cluster is not constant as expected. If this phenomenon is observed among red supergiants (RSG, see Sec. 2.1), those massive stars are referred to as red stragglers. However, the same observation is made for the main sequence (MS) turnoff where they are called blue stragglers.
An example of such observations would be the VLT-FLAMES survey (N.Brivatsky et al. (2018)). The survey resulted in an estimated age spread of (12 - 22) million years for the RSGs in the cluster SL 639 , and in an age spread of (14 - 24) million years among the RSGs in the cluster Hodge 301 (Fig. 1.1). Both are stellar clusters in the Large Magellanic Cloud (LMC).
It is suggested that this phenomenon could be explained by binary evolution (N.Brivatsky et al. (2018)) and we want to test this theory based on a grid of simulated binary systems with LMC properties.

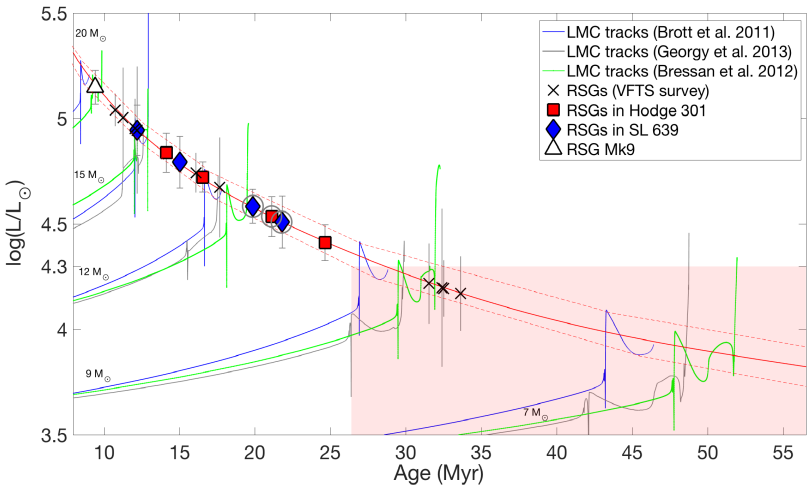

Figure 1.1: Age-luminosity diagram used to estimate the age of the RSGs in the stellar clusters Hodge 301 and SL 639 (N.Brivatsky et al. (2018). The luminosity of the RSGs is compared to theoretical age-luminosity tracks to estimate the age.

1.2 The influence of binary evolution on supernova progenitors

Recent observations have shown that a large fraction of massive stars, 50 % or more, will be influenced by interacting with a binary companion during their evolution (Sana et al. (2012b), Sana et al. (2013), Sana et al. (2012a)). This is why binary evolution cannot be ignored when studying RSGs. Since many RSGs are expected to explode as a supernova at the end of their lifetime the question arises, how supernovae are influenced by the previous binary interaction of the progenitor. There is so far no detailed observational or theoretical work on how RSG supernova progenitors are influenced by binary evolution. They are suggested to be the progenitors of type IIP supernovae (see Sec. 2.3, Smartt (2009)). However, the possibility that an influence is apparent can not be outruled (Smartt (2009)). For this thesis we made an approach to determine, how the final properties of a RSG before its explosion could be influenced by previous binary interaction.

Chapter 2

Physics

2.1 Massive stars on the RGB

We use stellar models with initial masses ranging from 10 $M_\odot$ to approximately 40 $M_\odot$ (see Sec. 3.1). These stars fall into the category of massive stars (O.R.Pols (2009)). As they reach the end of their main sequence life, they will expand their envelope as they start burning hydrogen in a shell around the core, moving on to helium burning in the core. During this phase they are very cool and luminous due to the inflated envelope and referred to as red supergiants (RSG). In a Hertzsprung-Russel diagram (HRD) their population is found on the red giant branch (RGB). After the end of the main sequence life all evolutionary developements take place at a much smaller timescale than hydrogen burning.
Stars that are more massive than 40 $M_\odot$ are expected to lose their envelope and become blue helium stars not entering the RGB (O.R.Pols (2009)). Although we do not have stars with an initial mass this high, a merger could result in a star more massive than 40 $M_\odot$.
RSGs have deep convective envelopes and therefore occupy an almost vertical line in the HRD along the Hayashi line. We can therefore assume that all RSGs have almost the same effective temperature (T_{eff}).

2.2 Binary Systems

2.2.1 Roche-Lobe overflow

The Roche potential, defined by Z. Kopal (Kopal (1955)), is formed by the combination of the gravitational potential of a star and the centrifugal force acting on the matter bound by a star in a binary system. As long as the material of a star stays within its Roche radius, it stays bound by the star. If the Roche radius is exceeded, mass transfer to a binary companion may happen.

2.2.2 Cases of Mass Transfer

In the literature the different cases of mass transfer are classified by the phase of evolution in which they take place. If mass transfer is already taking place when both stars are still on the main sequence, it is called it Case A mass transfer.
In many cases mass transfer sets in as the primary star moves to the RGB inflating its envelope. This case is referred to as Case B mass transfer. Case A mass transfer that does not result in a merger is always followed by Case B.
In some rare cases mass transfer happens only after the primary depleted helium. We call it Case C mass transfer. Whereas mere Case C mass transfer is rare, it follows after Case B mass transfer quite often.
At primary masses up to approximately 20 $M_\odot$ some systems with large periods and mass ratios between 0.975 and 0.4 never undergo mass transfer. These systems are referred to as non-interacting binary systems. In this case both stars evolve like single stars.
Note that the primary star is defined as the star that loses mass to its companion first even if inverse mass transfer might set in later.

In many cases the mass transfer rate grows large enough for the system to become unstable. If this happens, the system is expected to merge and form a new single star.

2.2.3 Late evolution of massive binaries

To determine wether stars in a binary system will move on to the RGB or not, we have to consider different scenarios.

- **Stable mass transfer:** In a system that undergoes stable mass transfer both companions can potentially become RSGs. For secondaries it is very common but most primaries, that have already lost an amount of hydrogen, will move towards becoming blue in their later evolution.
- **Merging during the MS:** A merger that happens when both stars are still on the main sequence will result in a new main sequence star. Just as for single stars, it depends on the mass wether the star will become a RSG or not.
- **Merging after the MS:** If the merger happens after the primary has depleted hydrogen, the convective cores won't be able to mix and a star with small helium core and massive envelope will be formed. This type of star will become blue instead of red and can be discarded for our project.
- **Common envelope:** Instead of a merger, that forms a new star, there is also the possibility of a scenario where the stars eject their envelopes during the process. For this work, this case is also not of interest, because no RSG will appear.

2.3 Supernovae IIP

In this work, we will also take a look at the final stadium of massive stars in a binary system. Many stars who populate the RGB and finished carbon burning are expected to explode as supernova (SN) after burning heavier elements up to iron in their core very rapidly (O.R.Pols (2009)). The SN is then classified by its spectral lines and developement of its brightness. The pre-SN structure of a star has a heavy influence of the type of SN that it will explode as. Since we focus on RSGs, we are most interested in Type IIP SNe, which are assumed to originate from the explosion of a RSG (Smartt (2009)). Type IIP SNe show hydrogen spectral lines and have a plateau phase in their luminosity as a function of time. The plateau exists due to recombination of hydrogen from the envelope of the progenitor star. The more massive the envelope is the longer the plateau phase lasts (O.R.Pols (2009)).

Chapter 3

Method

3.1 Properties of the data grid used for our study

For our study we use a grid of evolutionary models of binary systems calculated by Pablo Marchant (P. Marchant Campos (2016)) with the MESA code (Modules for Experiments in Stellar Astrophysics). The masses of the primary stars (M_1) are in a range from 10 $M_\odot$ to 40 $M_\odot$ in logarithmic steps of 0.05. The mass ratio of primary and secondary ($q = \frac{M_2}{M_1}$) goes from 0.25 to 0.975 in steps of 0.025. The orbital period (P) of the binary system is in range of $log(P) = 0.15$ (≈ 1.4 days) to $log(P) = 3.5$ (≈ 10 years) in steps of 0.05 (by $log(x)$ we always refer to a logarithm to the base 10). All stars are calculated until carbon depletion if no merger happens (see Sec. 2.2.2).
To have single stars as a comparison we use non-interacting binaries for the lower mass range.For more massive single stars we use models calculated after the models of Pablo Marchant by Nathan Grin. We need those additional models, because there will be no non-interacting models available from the binary grid at higher masses.
All models are calculated with the initial chemical composition of the Large Magellanic Cloud.
Mass transfer is realised by Roche-lobe overflow.
As criterion for convection the Ledoux criterion is used. Apart from that, the mechanisms of thermohaline mixing, rotational mixing and semi-convection are included. Further, the calculation takes tidal effects and transfer of angular momentum during mass transfer into account.It is also assumed that the rotational velocities of two stars in a binary system are tidally synchronized as the stars begin their main sequence life.
Note that if one star of the binary system depletes carbon, the other star will still be further developed as a single star until it reaches carbon depletion itself. For more detailed information we refer to P. Marchant Campos (2016) Ch. 5.1.

3.2 Assumptions for our simulations

In this study, we will simulate the RSG population in a stellar cluster with LMC properties (see Ch. 4). For binary systems we will draw random triples corresponding to primary star mass, mass ratio and orbital period and assign them to the closest data point in the grid.We do the same for single stars where we only draw random numbers for the star mass. To take the star formation conditions into account, the primary and single stars in all simulations are weighted with the salpeter initial mass function (IMF), which favours lower star masses.

$$p(M_1) \propto M_1^{-2.35}$$

We also favour closer binaries while the mass ratio distribution is almost flat (Sana et al. (2012b)).

$$p(log(P)) \propto log(P)^{-0.55}$$

$$p(q) \propto q^{-0.1}$$

We consider 50% of massive stars in a cluster to have a binary companion (Sana et al. (2013)).

3.3 Merger

If mass transfer occurs in a very close binary, or if the accreting star can not remain stable due to the infalling mass, a merger can occur. If both merging stars are still on the main sequence, a new main sequence star is born.
From the data grid we can expect a merger if both stars terminate their evolution at the same time. There are, however, different evolutionary scenarios that lead to a merger.For more detail on this we refer to P. Marchant Campos (2016). To determine the properties of a merger product we use a method proposed by Schneider et al. (2016). The mass and convective core of the merger product is calculated. Then we assign a single star to the merger product with the closest mass, core mass and a corresponding main sequence age.
During the merging process a fraction of the stellar material is lost. This fraction is taken into account by the factor

$$\Phi = \frac{0.3\, q_{merge}}{(1+q_{merge})^2}.$$

q_{merge} is the mass fraction of the binary system at the time of merging. Then we can calculate the total mass of the merger product with

$$M_{tot} = (1-\Phi)(M_1 + M_2).$$

For further proceeding, we have to extrapolate the main sequence lifetime and mass as well as hydrogen mass fraction at the end of the main sequence.
Then the size of the convective core is $\frac{\langle X\rangle}{X_0}$ (where $\langle X\rangle$ is the average hydrogen mass fraction of the whole star at the time of merging and X_0 is the initial hydrogen mass fraction). It can be calculated as

$$\frac{\langle X\rangle}{X_0} = \frac{(1-Q_{m,1}f_1)(1-Q_{c,1}f_1-\Phi)}{(1-\Phi)[(1-Q_{m,1}f_1)+(1-Q_{m,2}f_2)q_{merge}]} + \frac{(1-Q_{m,2,f_2})(1-Q_{c,2}f_2-\Phi)q_{merge}}{(1-\Phi)[(1-Q_{m,1}f_1)+(1-Q_{m,2}f_2)q_{merge}]}.$$

Here $Q_{m,i}$ is the mass fraction that the star with mass M_i loses on the main sequence, $Q_{c,i}$ is the effective core mass fraction of the star with mass M_i, and f_i is its fractional main sequence age at the time of merging.
We can calculate $Q_{m,i}$ and $Q_{c,i}$ with

$$Q_m = \frac{M_{ini} - M_{TAMS}}{M_{ini}},$$

$$Q_c = \frac{X_0 - \langle X\rangle_{TAMS}}{X_0}$$

where M_{TAMS} and $\langle X\rangle_{TAMS}$ are the mass and hydrogen mass fraction at the end of the main sequence we get from our extrapolation. Then the apparent main sequence age of the newly formed star is

$$f_{app} = \frac{f_i}{\alpha}.$$

f_i is the fractional main sequence age of a corresponding single star and α is a factor that accounts for additional mixing. In our case we take $\alpha = 1.14$ (Schneider et al. (2016)).

Chapter 4

The luminosity distribution of RSGs

We simulate the RSG population of a stellar cluster consisting of 200.000 systems taking the assumptions of section 3.2 into account. We will look at the luminosity distribution of RSGs in the cluster at a fixed age to find out wether it is influenced by binary evolution. We simulate the cluster from 6 Myr to 26.1 Myr in steps of 0.3 Myr. As a criterion for the star being a RSG we require the star to have depleted hydrogen to the point where the mass fraction of hydrogen in the core lies under 1 %. Further, the effective temperature (T_{eff}) of the star has to be below $log(T_{eff}) = 3.7$. This temperature is still fairly hot for a RSG and we may have to make further restrictions for young clusters.

4.1 Analytical estimate for single stars

We can already estimate the luminosity spread of single stars on the RGB. The spread is determined by two factors. One is the spread in masses that populate the RGB at a fixed time. The other is the change in luminosity of a single star during the RGB phase.
To estimate the effect of the first factor we assume that a star spends about $\frac{1}{10}$th of his lifetime on the RGB. So for two stars to still be together on the RGB, the MS lifetime of the less massive star can only be as much longer as the MS lifetime of the more massive star, as the more massive star stays on the RGB. In combination with the relation between mass and MS-lifetime $\tau \propto M^{-2}$ we get a constant spread in mass of 4.8%.
For the maximum change in luminosity on the RGB for a star of a certain mass we make a linear fit using age-luminosity tracks of RSGs used by N.Brivatsky et al. (2018) (Fig. 1.1).We take the maximum and minimum luminosity during the RSG phase for each curve and fit is as a function of the mass.
The maximum luminosity width is then between the most massive star at maximum luminosity and the least massive star at minimum luminosity. Using the mass-MS-lifetime relation we can relate this width to the age of the cluster. As a function of the cluster age the luminosity develops as shown in Fig. 4.1.The plot depicts the width in logarithmic luminosity divided by the mean logarithmic luminosity.
However, it is probably not likely to observe the full spread, because the luminosity changes on a small timescale during this phase of stellar evolution. One would have to observe exactly, when the most massive star is at maximum luminosity and the least massive star is at minimum luminosity. The estimate is therefore to be seen as an upper limit.

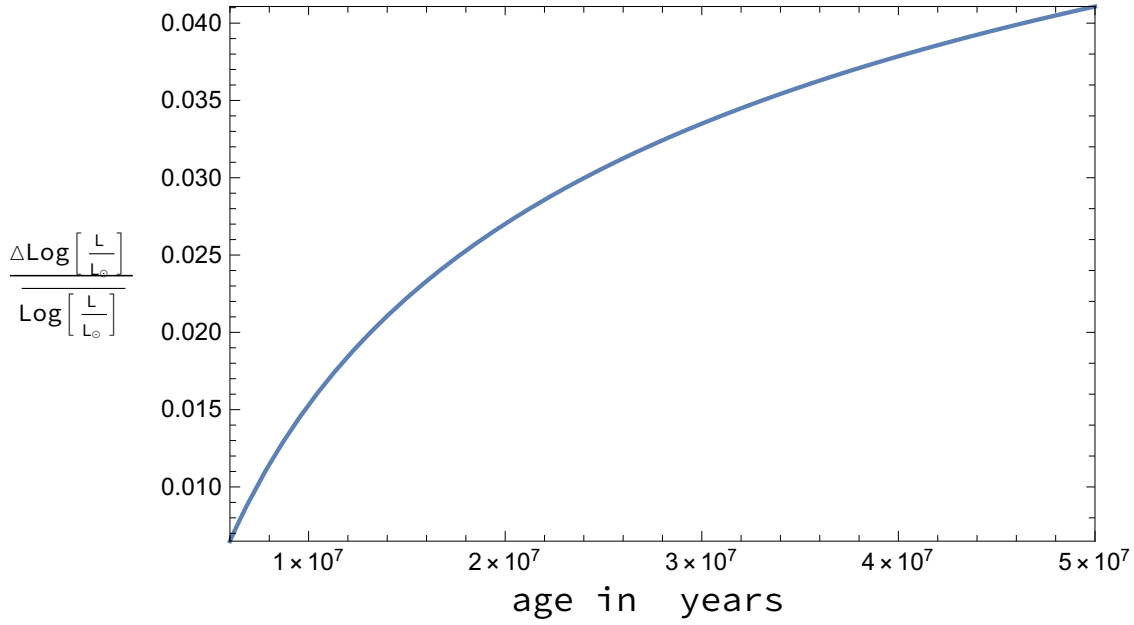

Figure 4.1: The plot depicts the relative spread of luminosity $\frac{\Delta log(\frac{L}{L_\odot})}{log(\frac{L}{L_\odot})}$ for single stars as a function of the age of a stellar cluster.

4.2 Accordance of the single star distribution with our analytical estimate

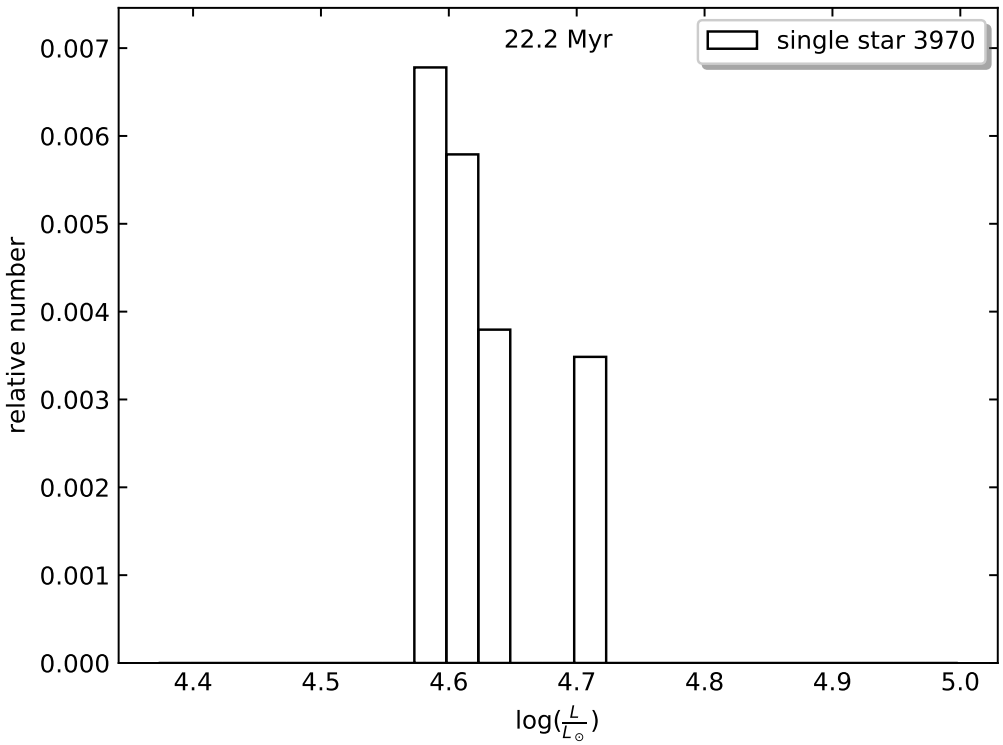

Figure 4.2: Luminosity distribution of single stars in the RSG phase in a stellar cluster of 22.2 Myr.On the y-axis is the total number of single star RSGs in a luminosity bin divided by the number of stars in the cluster. The legend gives the total number of single star RSGs.

To test our simulation, we can compare the estimated spread of luminosities for single stars with the results. It is, however, the case that our grid is less dense for massive single stars than for less massive ones. So the distribution is in most cases narrower than estimated if we look at clusters up to 16.2 Myr.
For the older clusters this effect does not play much of a role. So we can use those to compare with the analytical estimate. The grid is still not continuous though, so to observe the full spread at all times remains unlikely.
This also shows, when we look at our distributions (see Appendix). The maximum spread of our distributions is in good accordance with the estimated upper limit.
In Fig. 4.2 we see the single star distribution that has the largest relative spread of our distributions, which is at 22.2 Myr. The estimated spread for 22.2 Myr would be ≈ 2.9 %. The spread of the simulated cluster lies at ≈ 3.2 %.

4.3 Influence of binary evolution on the luminosity distribution

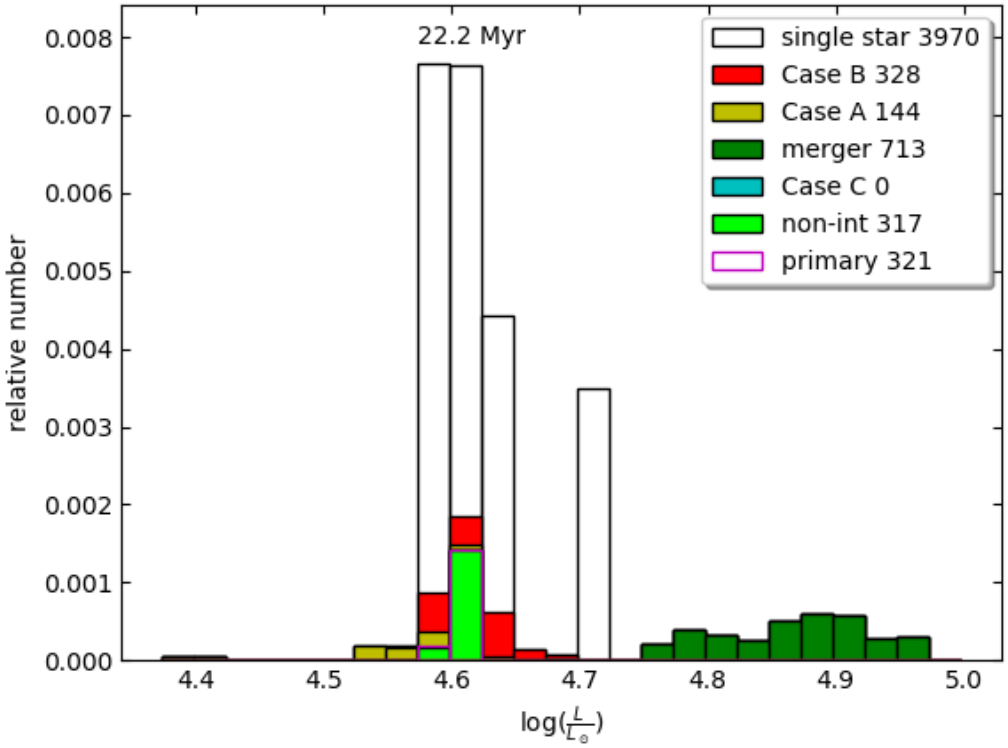

Figure 4.3: Luminosity distribution of all stars in the RSG phase in a stellar cluster of 22.2 Myr. On the y-axis is the total number of RSGs in a luminosity bin divided by the number of stars in the cluster. The legend gives the total number of RSGs of the designated type.

If we look at the same cluster with the distribution of binary systems added, the luminosity distribution is as shown in Fig. 4.3.
There are two apparent features. The single star peak appears to be slightly widened if the luminosity distribution of stable mass transfer systems is added, this feature is rather small though and probably not observable. There is also a spread towards higher luminosities caused by mergers.
In this plot, there are also some mergers at lower luminosities. These are mergers that are transitioning to the RGB in this moment. The transition phase is very short and is not included in our analytical estimate for the luminosity width, however, in this case it is apparent (see Fig. 4.4).

Two aspects should always be kept in mind while looking at our results, the discrete data grid and the very sharply defined time at which we look at the cluster. If the luminosity of a system in the grid is at a maximum or minimum when we look at it, this luminosity will appear in the distribution even if it is only a very short-lived state. The discrete data grid can cause gaps and discretisation in our distributions.

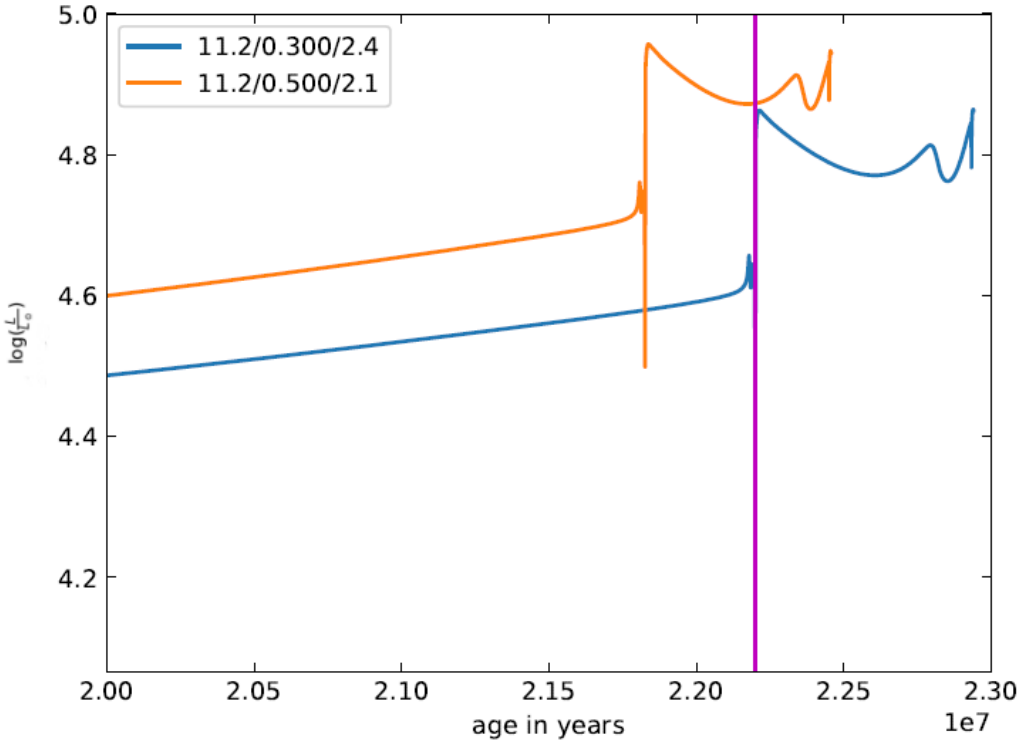

Figure 4.4: Age-luminosity diagram for two RSGs that are merger products;one of them is transitioning to the RGB at exactly 22.2 Myr, which shows in the distribution.The legend shows the properties of the single star the merger product is assigned to by *'initial primary mass/mass ratio /period in days'*.The pink line is at 22.2 Myr.

4.4 Comparison with observed clusters

The luminosity spread caused by mergers appears to be similar to the red straggler effect. To compare our simulation with observations, we can compare the age spread suggested by mergers with the observed age spreads of SL 639 and Hodge 301.
Therefore, we look at clusters at the age of 22 Myr (Fig. 4.5) and 24 Myr (Fig. 4.6). Those are the upper age limits estimated for SL 639 and Hodge 301.
Then we look for a system that has its single star peak at the luminosity of the most luminous merger.
The most luminous merger in a 22 Myr old cluster has a luminosity of $log(\frac{L}{L_\odot}) = 5.0$. For a cluster of 24 Myr it is $log(\frac{L}{L_\odot}) = 4.9$.
If these mergers were to be regarded as normally born single stars, they would suggest an age of (12.9 - 13.8) Myr ($\pm$ 0.3 Myr) for $log(\frac{L}{L_\odot}) = 5.0$ (Fig. 4.7). For $log(\frac{L}{L_\odot}) = 4.9$ it is (14.1 - 15) Myr ($\pm$ 0.3 Myr) (Fig. 4.8).
This corresponds to an age spread of (9.4 - 7.9) Myr for a cluster of 22 Myr (like SL 639) and to an age spread of (10.2 - 8.7)Myr for a cluster of about 24 Myr (like Hodge 301).
These values correspond quite nicely with the estimated age spread of 10 Myr from the observations.
It is also apparent that the distributions look fairly different despite the age being similar. This is a consequence of the aspects mentioned in Sec. 4.3. Our grid is discrete and luminosity changes on a small timescale during the RSG phase, so the distributions can look differently even for small timesteps.

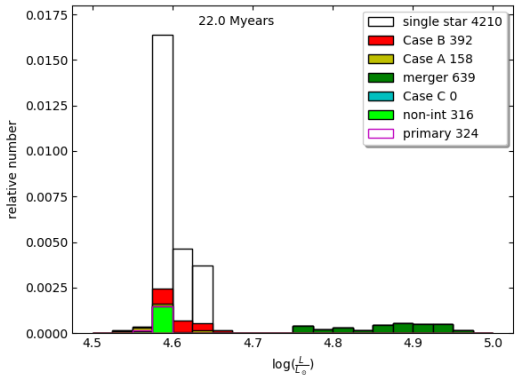

Figure 4.5: As in Fig. 4.3, but for an age of 22 Myr

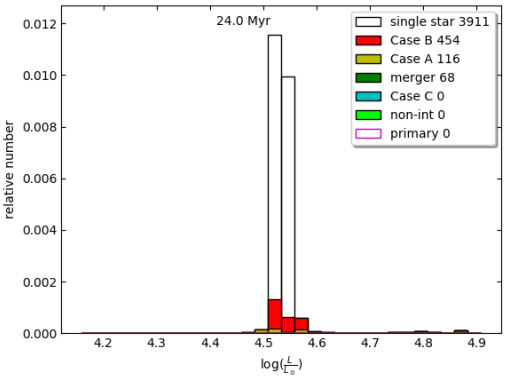

Figure 4.6: As in Fig. 4.3, but for an age of 24 Myr

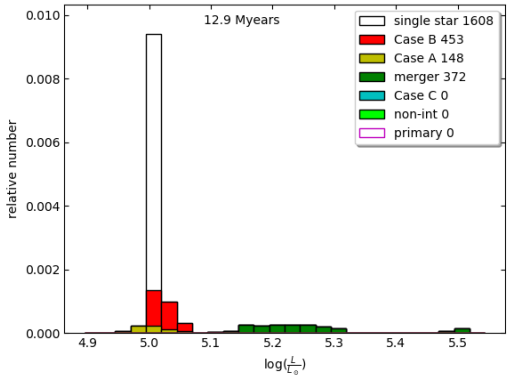

Figure 4.7: As in Fig. 4.3, but for an age of 12.9 Myr

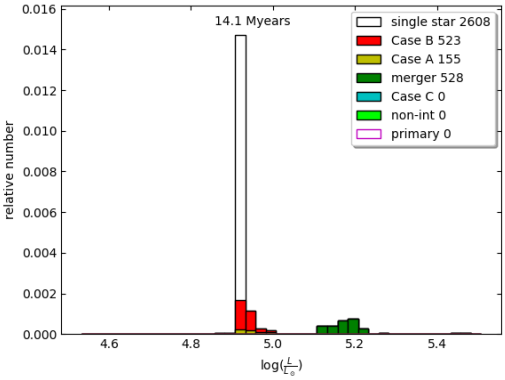

Figure 4.8: As in Fig. 4.3, but for an age of 14.1 Myr

4.5 Scale of the influence

Now we want to see how many red stragglers we should expect in a stellar cluster. Therefore we look at different ratios as a function of time (see Fig. 4.9).All of them refer only to RSGs.
First, we have the ratio of mass gainers to non-interacting binaries and single stars.Under the designation 'mass gainers' are all stars included that either accreted mass through stable mass transfer or gained mass during a merging process. There is further the ratio between merger products and stars in a binariy that did not merge but went through stable mass transfer or did not interact. At last, there is the ratio between merger products and single stars and the ratio between merger products and the total number of RSGs. To calculate the curves we take the distribution of the luminosity for RSGs from 6 Myr to 26.1 Myr in steps of 0.3 Myr. Then the ratios mentioned before are calculated for each age.
Again the effects of the discrete grid have an impact. The effect is especially high on the number of merger products.It results in maxima where a lot of merger products originating from the same primary star mass are apparent and corresponding minima. That is why we also calculate the mean value over time (see Tab. 4.1).

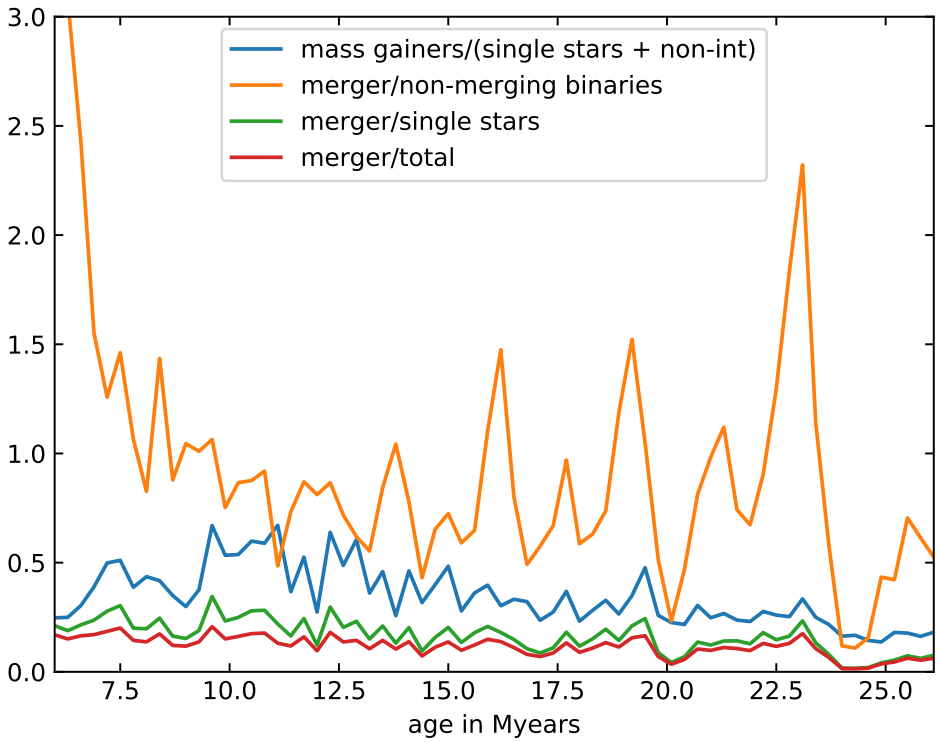

Figure 4.9: All ratios depicted refer to RGSs.On the x-axis is the age of the cluster in units of million years. On the y-axis is the ratio of systems designated in the legend.

Table 4.1: Table of the mean values depicted in Fig. 4.9.

$\frac{\text{mass gainer}}{\text{single stars + non-int}}$	0.34
$\frac{\text{merger}}{\text{non-merging binaries}}$	0.98
$\frac{\text{merger}}{\text{single stars}}$	0.16
$\frac{\text{merger}}{\text{total}}$	0.12

It is originally assumed, that 50 % of all systems are binaries, however, not all of them become RSGs so we have a lower mean value of binaries and single stars of 36 %, at certain times the value can go above 50 % though.
The ratio of merging and non-merging binaries is heavily influenced by grid effects, the mean value suggests that there is approximately the same number of merging and non-merging systems.
The mean value of the ratio of mergers compared to all systems lies at 12 %. This is very close to the portion of mergers we can estimate from the grids. It is a bit surprising, that the value is not higher, because they are preferred by our weighting. The maximum of the curve lies at approximately 20 %. This is still under the estimated maximum ratio of blue stragglers, that lies at 30 % (N.Brivatsky et al. (2018)). An observational estimate for red stragglers explicitly has not yet been derived from observations, because there are very few RSGs per cluster observed.

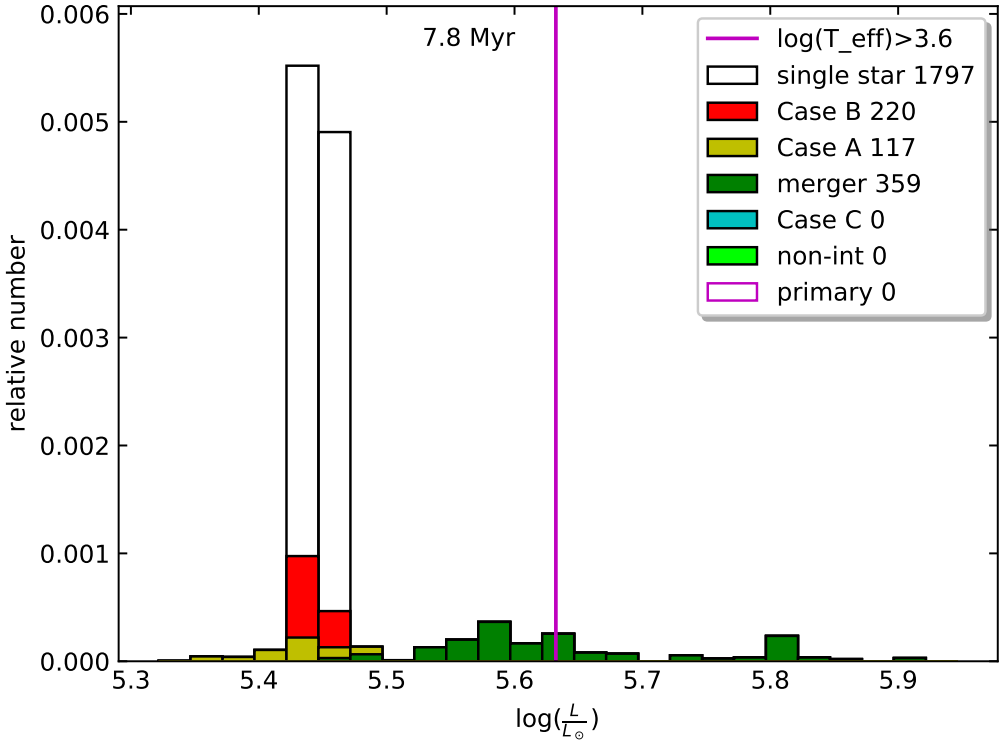

Figure 4.10: As in Fig. 4.3, but for an age of 7.8 Myr; the pink line marks the threshold to stars hotter than $log(T_{eff}) = 3.6$.

4.6 Further restriction for young clusters

In very young clusters some massive luminous mergers will appear in our distribution. Their effective temperature is very close to the upper limit we set. For some of them it might be not entirely clear if they should still be called RSGs.
In Fig. 4.10 is an example for a cluster of 7.8 Myr. The mergers on the right side of the pink line are hotter than $log(T_{eff}) = 3.6$ and might not necessarily be labeled as RSGs.
This lowers the upper luminosity that would be observed.

Chapter 5

Distribution of pre-SN properties

We will simulate a sample of 200.000 systems again. The simulation is made under the same assumptions as before (see Sec. 3.2). This time we will look at the sample of stars at the moment of carbon depletion, regardless of age, under the condition that they are RSGs at this point.Because the time between carbon depletion and core collaps is so short, we can assume that the properties of a star at this point are critical for the properties of its supernova. We will plot the distribution of final radius, core mass and envelope mass, as well as initial mass within a fixed luminosity range of $\Delta log(\frac{L}{L_\odot}) = 0.05$.

5.1 Analytical estimate of the radius distribution for single stars

At least for the radii we can make an estimate beforehand. As mentioned in Sec. 2.1 the stars on the RGB are very close to the Hayashi line. So they occupy a very narrow range in effective temperature. This allows us to estimate the spread of final radii within a fixed luminosity range using the Stefan-Boltzmann-Law

$$L = 4\pi R^2 \sigma T^4.$$

For a luminosity range of $\Delta log(\frac{L}{L_\odot}) = 0.05$ this results in a radius spread of ≈ 5.5 %. This value is the width of radii divided by the mean value.

5.2 Distribution of the final effective temperature

First we can take a short look at the final distribution of the effective temperature to test our assumption made in Sec. 5.1. The distribution is shown in Fig. 5.1. As we can see the distribution is very narrow and spreads only within the order of the third digit. Therefore, our assumption for the estimate of the final radius can be seen as valid.

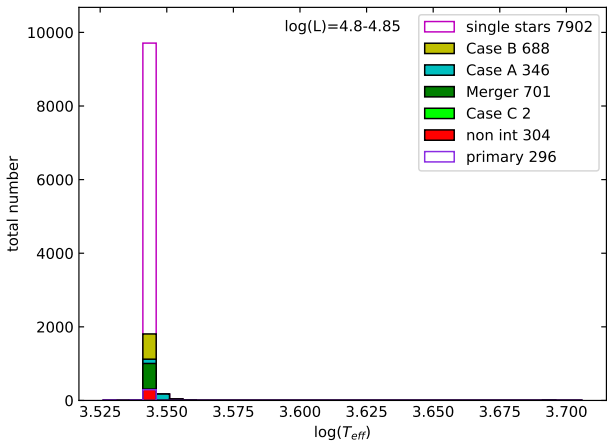

Figure 5.1: Distribution of the effective temperature at the moment of carbon depletion for RSGs with luminosities in the range $log(L)$ = 4.8 - 4.85; on the x-axis is the logarithmic effective temperature in Kelvin. On the y-axis is the total number of RSGs in a temperature bin.

5.3 Distribution of the final radius

If we now look at the distribution, that our simulation results in (Fig. 5.2), we can first compare it with our analytical estimate and then look at the influence of binary evolution.
The spread of radii for single stars amounts to approximately 5.9 % which is in accordance with our estimate. If we include the binary systems but ignore the extreme outliers, the spreads grows to to 8.8 % which is still a very moderate deviation.

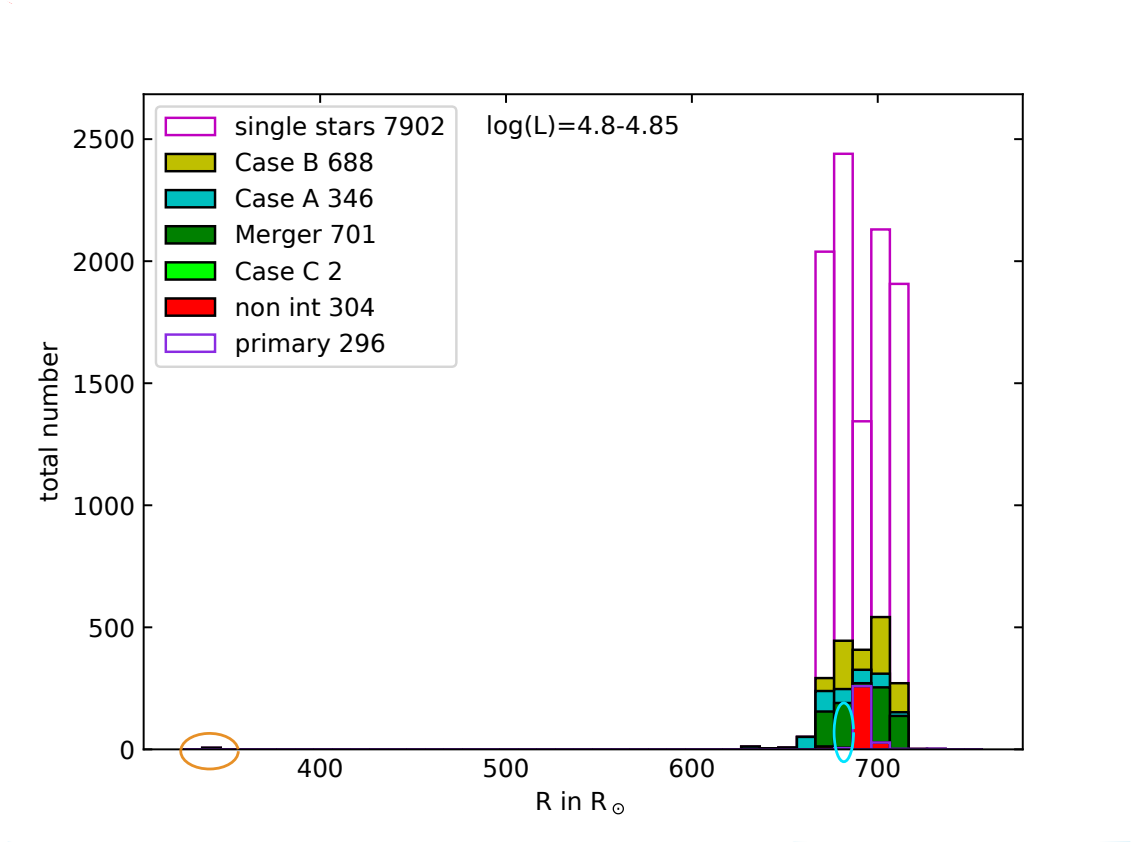

Figure 5.2: As in Fig. 5.1, but for the final radius distribution. The circled bins are the bins in which the systems lie that will be further illustrated.

There are a few systems that lie very far from the single star distribution. If we look a bit deeper into them, we find that those are systems which either go through a blue loop or burn helium as a blue star.Those systems only expand their radius and become red shortly before carbon depletion. They deplete carbon while still expanding and therefore have a smaller radius than expected.
In Fig. 5.3 the age-radius diagrams of two systems that contribute to the distribution are shown. Both tracks end at carbon depletion. It is apparent that one of the systems depleted carbon during its expansion. This phenomenon, however, is not the result of binary evolution.

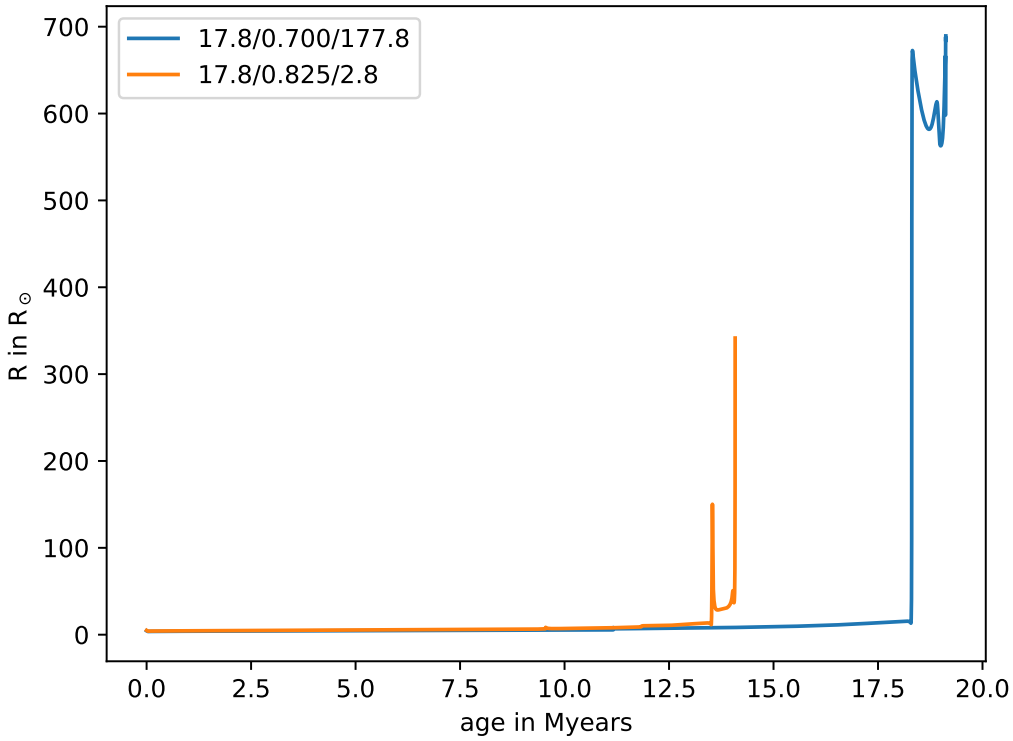

Figure 5.3: Radius as a function of age for two systems in the bins marked in Fig. 5.2 in the corresponding colour.The legend shows the properties of the systems by *'initial primary mass/mass ratio /period in days'*.

5.4 Distribution of the final core mass

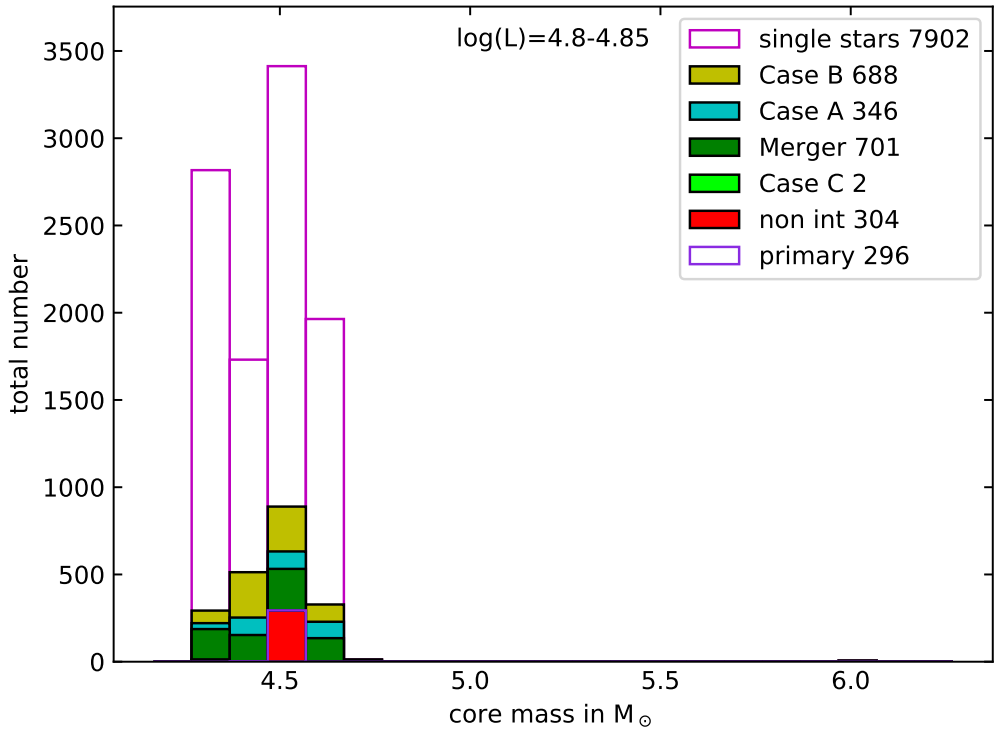

Figure 5.4: As in Fig. 5.1, but for the final core mass distribution.

The result for the final core masses is similar to the result for the final radii (Fig. 5.4). Here the spread for the single stars lies at approximately 5.8 % and including binaries 7.2 %. There is no strong feature caused by binary evolution apparent either.

5.5 Distribution of the final envelope mass

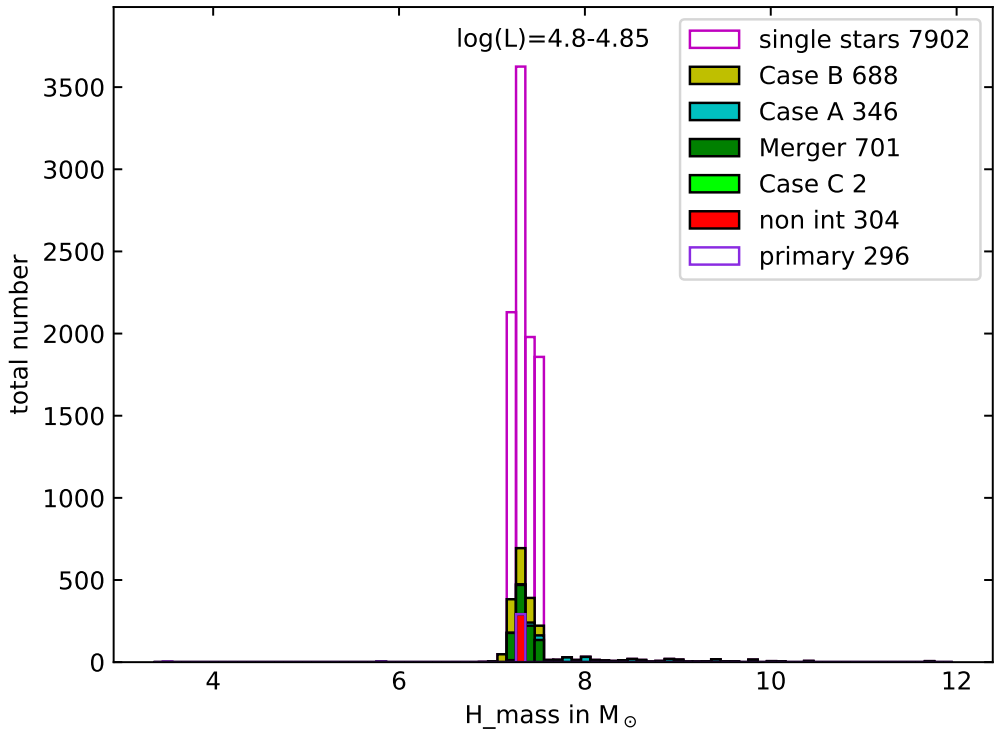

Figure 5.5: As in Fig. 5.1, but for the final envelope mass distribution.

If we look at the at the distribution of the final envelope mass (Fig. 5.5), there is an apparent feature caused by binary interaction. Here we can see a spread towards higher envelope masses caused by systems that underwent Case A mass transfer.
If we take a closer look at them, they consist of binary systems with high mass ratios and low periods.
This can be explained by the similar paced evolution that primary and secondary have in this case. The mass will be transferred to the secondary at a time where the hydrogen burning is already relatively far advanced, so that there will be a lot of helium in the core. In this case the chemical gradient between core and envelope will be rather steep preventing the hydrogen to mix in the core via convection. So it will remain in the envelope leading to a star that has an envelope too massive for its core (Braun, 1997).
This is illustrated in Fig. 5.6. A star that accretes during an early phase of hydrogen burning has a hydrogen profile very close to that of a single star. If there is already a high abundance of helium in the core, the gradient between envelope and core becomes very steep.

We would suggest these type of stars to be progenitors of type IIP SNe that have an unexpectedly long plateau phase for their respective core mass.
To make an estimate for the scale of the effect, we can plot the ratio of systems that have an especially massive envelope compared to the total number of RSGs in a luminosity bin (Fig. 5.7). As a criterion for the envelope to be especially massive we choose a deviation from the mean value for single stars of 10 %. It can be seen that the ratio of systems that have an especially massive envelope is not very high at most luminosities.
With an average ratio of approximately 2.3 % observational comparison could be difficult.

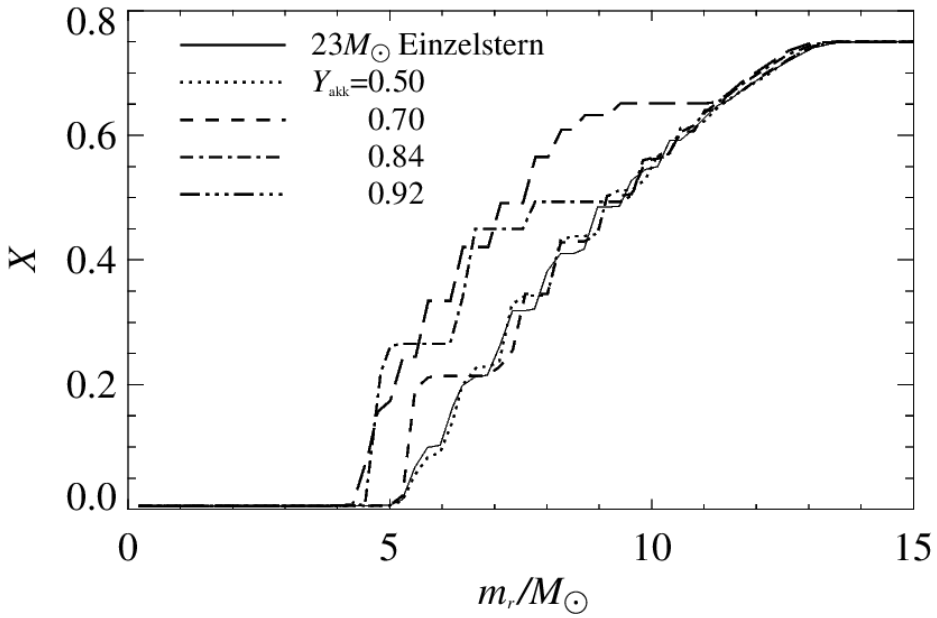

Figure 5.6: The graphic portays the hydrogen profile of a star of 20 $M_\odot$ that accretes 3 $M_\odot$ of hydrogen at different stages of hydrogen burning.For comparison there is also the profile of a 23 $M_\odot$ massive star.(Braun, 1997)

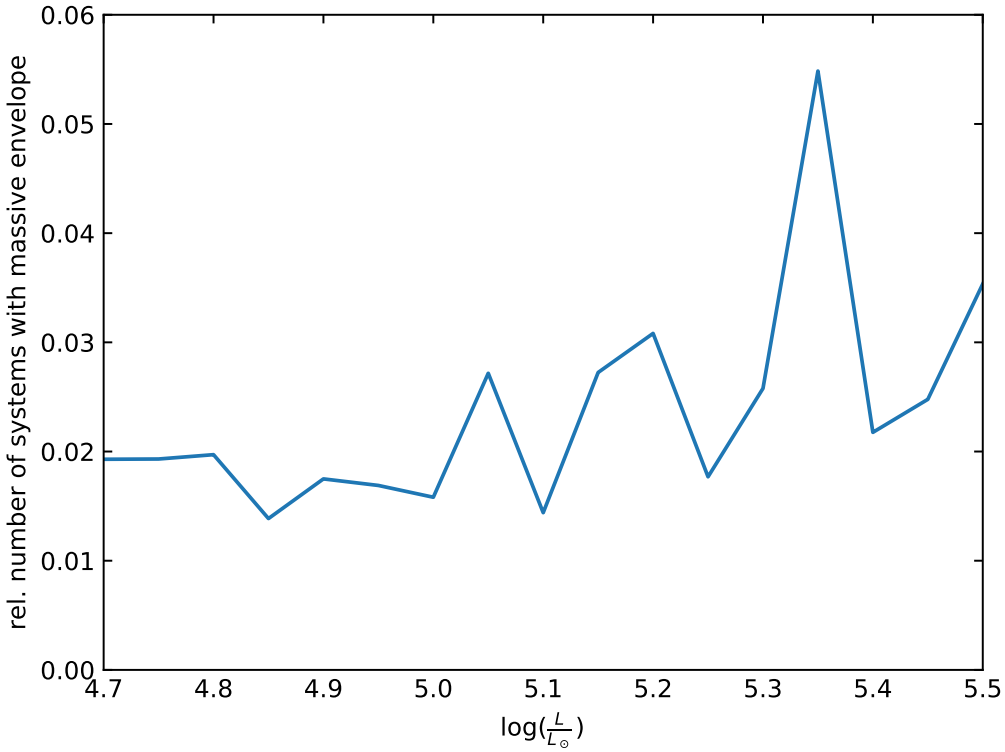

Figure 5.7: On the x-axis is the logarithmic luminosity in units of solar luminosity.On the y-axis is the number of systems with an especially massive envelope divided by the total number of systems in the respective luminosity bin.

5.6 Distribution of the initial mass

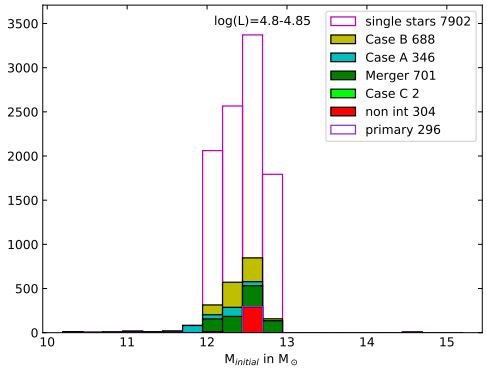

Figure 5.8: As in Fig. 5.1, but for the initial mass distribution.

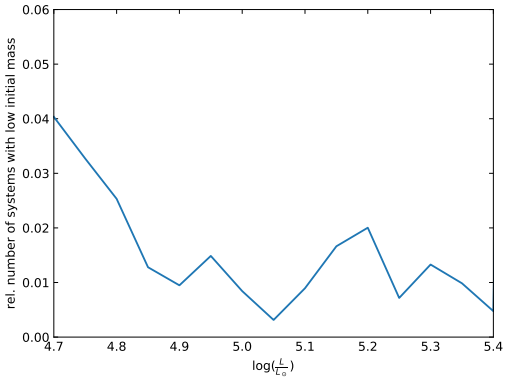

Figure 5.9: As Fig. 5.7, but for systems that have an especially high initial mass.

At last we will look at the distribution of initial masses of systems that deplete carbon at a certain luminosity (Fig. 5.8). Here a feature caused by Case A mass transfer is apparent again. There is a spread towards lower initial masses consisting of Case A systems. However, this time the tail consists of Case A systems with low mass ratios.For these systems the hydrogen can be mixed into the convective core and a star with a hydrogen profile close to that of a single star is formed.This way they have a higher final mass and matching core mass due to accretion.

Again, we can estimate the scale of the effect.We use the same criterion as in Sec. 5.5, this time the intial mass has to deviate more than 10 % from the mean value of the single star distribution. As Fig. 5.9 shows that the ratio of systems with an especially low initial mass is even lower than the ratio of systems with an especially massive envelope. Here the average ratio is 1.5 %. This might be due to the fact that a lot of systems with low mass ratio and orbital period end as a merger instead of undergoing stable mass transfer.

Chapter 6

Conclusion

Using the data grid of binary systems calculated by P. Marchant Campos (2016) we could simulate the luminosity distribution of RSGs in a stellar cluster for a constant age. It is apparent that stable mass transfer has only a minor effect on the distribution. However, there is a large spread towards higher luminosity caused by merger products. These luminous mergers suggest a younger age than the age of the cluster and are therefore possible candidates for red stragglers. Comparing the age spread of our simulation with the observational age spread shows that they are in good accordance.

We also looked at the final properties of RSGs at the moment of carbon depletion at constant luminosity and came to the result that neither the final radius nor the final core mass is heavily affected by binary evolution.
There is, however, a spread towards more massive final envelopes caused by system that received hydrogen through Case A mass transfer and did not mix it into the convective core. We assume that these systems would result in a type IIP supernova with a plateau phase too long for the suggested progenitor mass. The ratio of such systems compared to all RSG progenitors at the same luminosity is not very high with a maximum of approximately 5.5 %.
There is also a spread towards lower initial masses consisting of systems that underwent Case A mass transfer and mixed the received hydrogen into the convective core. Here again, the number of these systems is small compared to the total number of RSGs within the same luminosity range.

Bibliography

[1] N.Brivatsky, D.J.Lennon, L.R.Patrick, C.J.Evans, A. Herrero, N. Langer, J. van Loon, J. Clark, F. Schneider, L. Almeida, and W. Taylor. "The VLT-FLAMES Tarantula Survey XXX. Red stragglers in the clusters Hodge 301 and SL 639". submitted to: *Astronomy&Astrophysics*. 2018.

[2] *Multplicity of massive O stars and evolutionary implications*. 2012.

[3] H. Sana, A. de Koter, S. E. de Mink, P. R. Dunstall, C. Evans, V. Hénault-Brunet, J. M. Apellániz, O. H. Ramírez-Agudelo, W. D. Taylor, N. R. Walborn, J. S. Clark, P. A. Crowther, A. Herrero, M. Gieles, N. Langer, D. J. Lennon, and J. S. Vink. "The VLT-FLAMES Tarantula Survey VIII. Multiplicity properties of the O-type star population". In: *Astronomy&Astrophysics* (2013).

[4] H. Sana, S. E. de Mink, A. de Koter, N. Langer, C. J. Evans, M. Gieles, E. Gosset, R. G. Izzard, J. B. Le Bouquin, and F. R. N. Schneider. "Binary Interaction Dominates the Evolution of Massive Stars". In: *Science* (2012).

[5] S. J. Smartt. "Progenitors of Core-Collapse Supernovae". In: *Annual Review of Astronomy and Astrophysics* (2009).

[6] O.R.Pols. *Stellar structure and evolution*. 2009.

[7] Z. Kopal. "The classification of close binary systems". In: *Annales D'Astrophysique* (1955).

[8] P. Marchant Campos. "The impact of tides and mass transfer on the evolution of metal-poor massive binary stars". PhD thesis. Rheinische Friedrich-Wilhelms-Universität Bonn, 2016.

[9] F. R. N. Schneider, P. Podsiadlowski, N. Langer, N. Castro, and L. Fossati. "Rejuvination of stellar mergers and the origin of magnetic fields in massive stars". In: *Monthly Notices of the Royal Astronomical Society* (2016).

[10] H. Braun. "Mischprozesse und Nukleosynthese in den Komponenten massereicher enger Binärsysteme". PhD thesis. Ludwig-Maximilians-Universität München, 1997.

[11] T. Nakaoka, K. S. Kawabata, K. Maeda, M. Tanaka, M. Yamanaka, T. J. Moriya, N. Tominaga, T. Murokuma, K. Takaki, M. Kawabata, N. Kawahara, R. Itoh, K. Shiki, H. Mori, J. Hirochi, T. Abe, M. Uemura, M. Yoshida, H. Akitaya, Y. Moritani, I. Ueno, T. Urano, M. Isogai, H. Hanayama, and T. Nagayama. "The Low-Luminosity Type IIP Supernova 2016bkv with Early-Phase Circumstellar Interaction". In: *The Astrophysical Journal* (2018).

[12] S. Adscheid. "Stellar population synthesis based on dense grids of detailed binary evolution models". Rheinische Friedrich-Wilhelms-Universität Bonn, 2018.

List of Figures

Appendix A

Figures

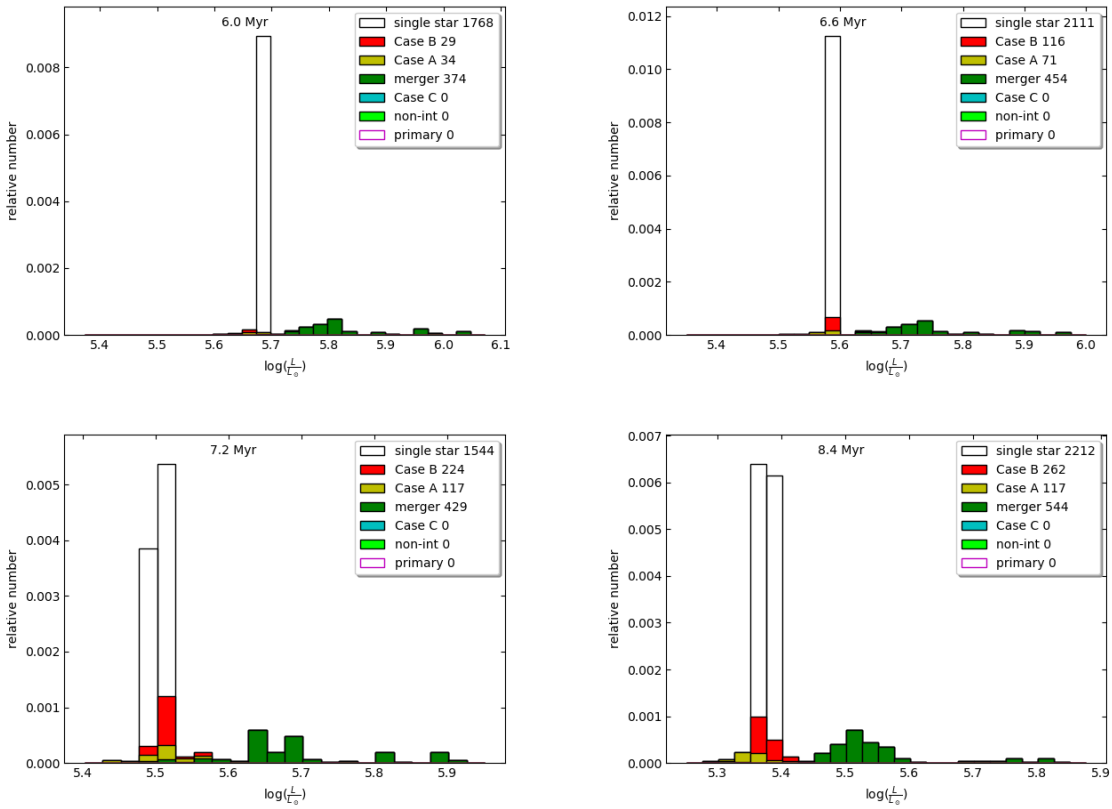

Figure A.1: Luminosity distribution of the RSG polulation of stellar clusters at the age of 6 Myr, 6.6 Myr, 7.2 Myr and 8.4 Myr

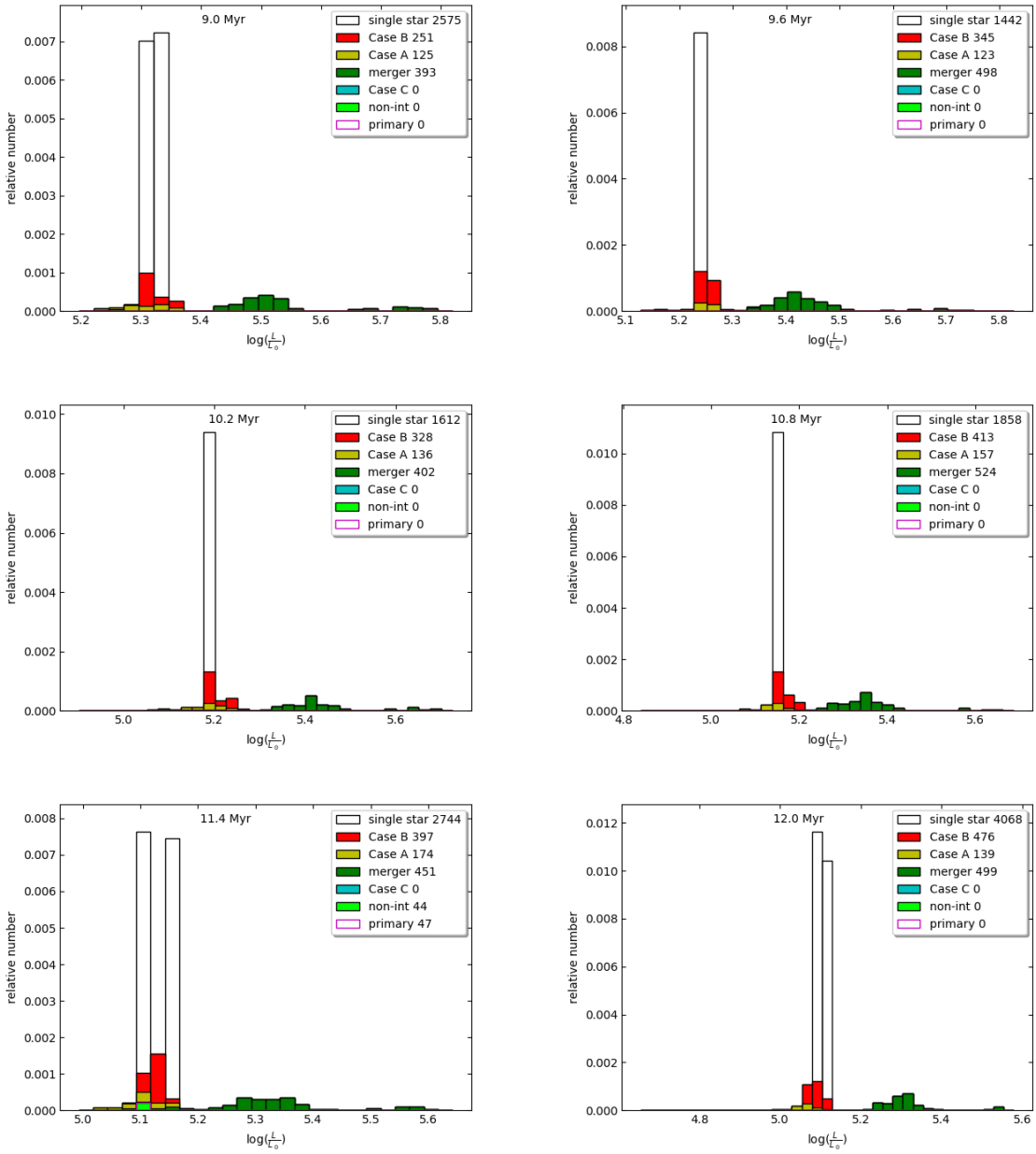

Figure A.2: As in Fig. A.1, but for ages of 9 Myr, 9.6 Myr, 10.2 Myr, 10.8 Myr, 11.4 Myr and 12 Myr

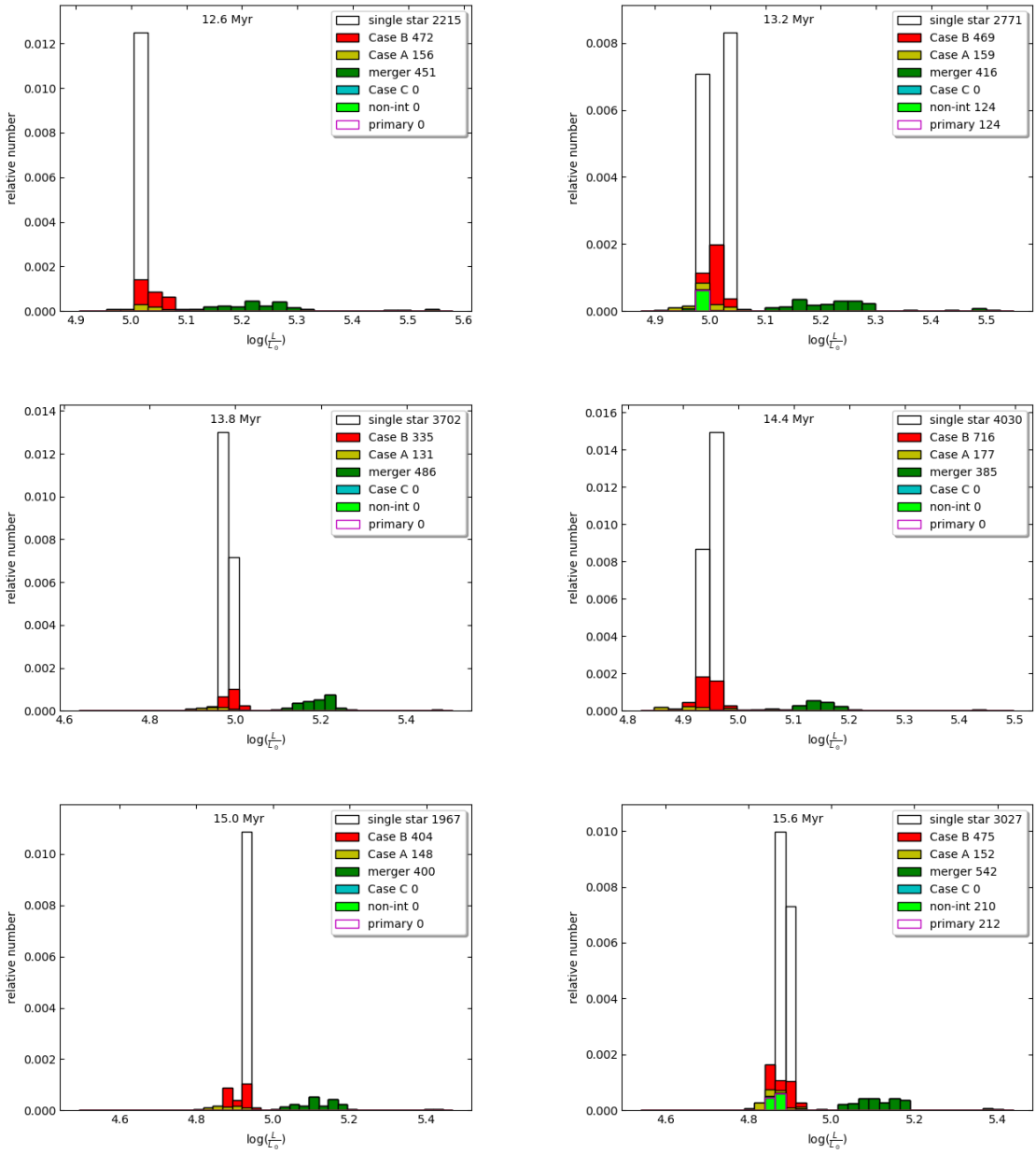

Figure A.3: As in Fig. A.1, but for ages of 12.6 Myr, 13.2, Myr,13.8 Myr, 14.4 Myr, 15 Myr and 15.6 Myr

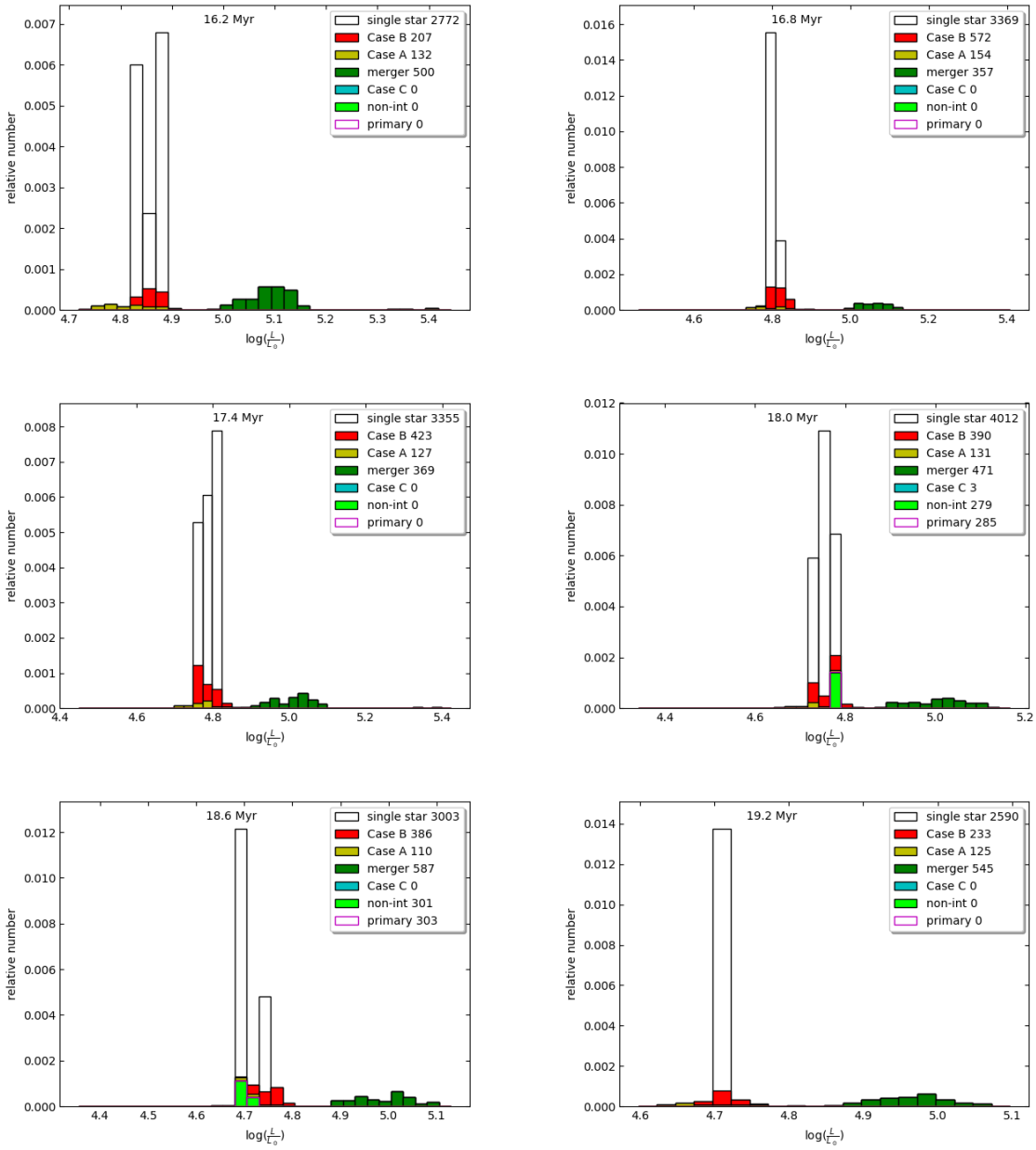

Figure A.4: As in Fig. A.1, but for ages of 16.2 Myr, 16.8, Myr,17.4 Myr, 18 Myr, 18.6 Myr and 19.2 Myr

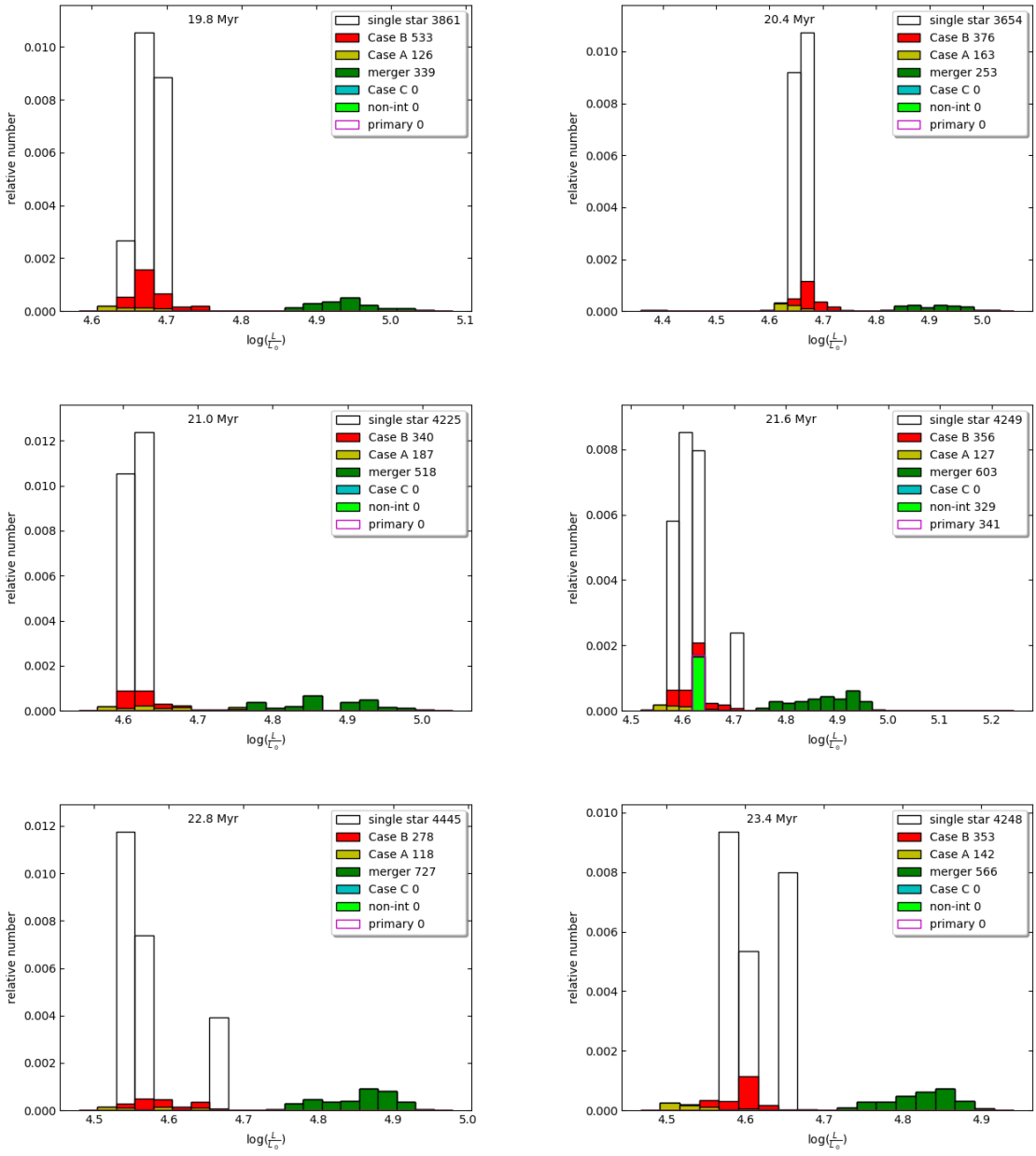

Figure A.5: As in Fig. A.1, but for ages of 19.8 Myr, 20.4 Myr, 21 Myr, 21.6 Myr, 22.8 Myr and 23.4 Myr

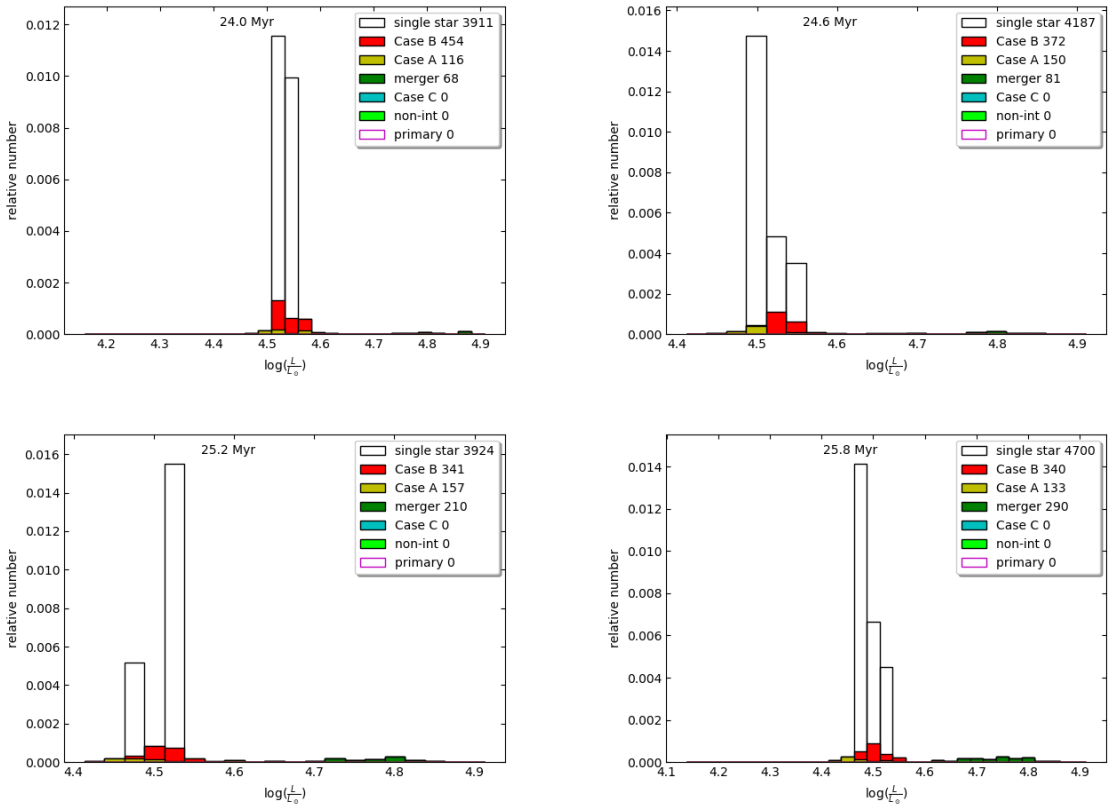

Figure A.6: As in Fig. A.1, but for ages of 24 Myr, 24.6 Myr, 25.2 Myr and 25.8 Myr

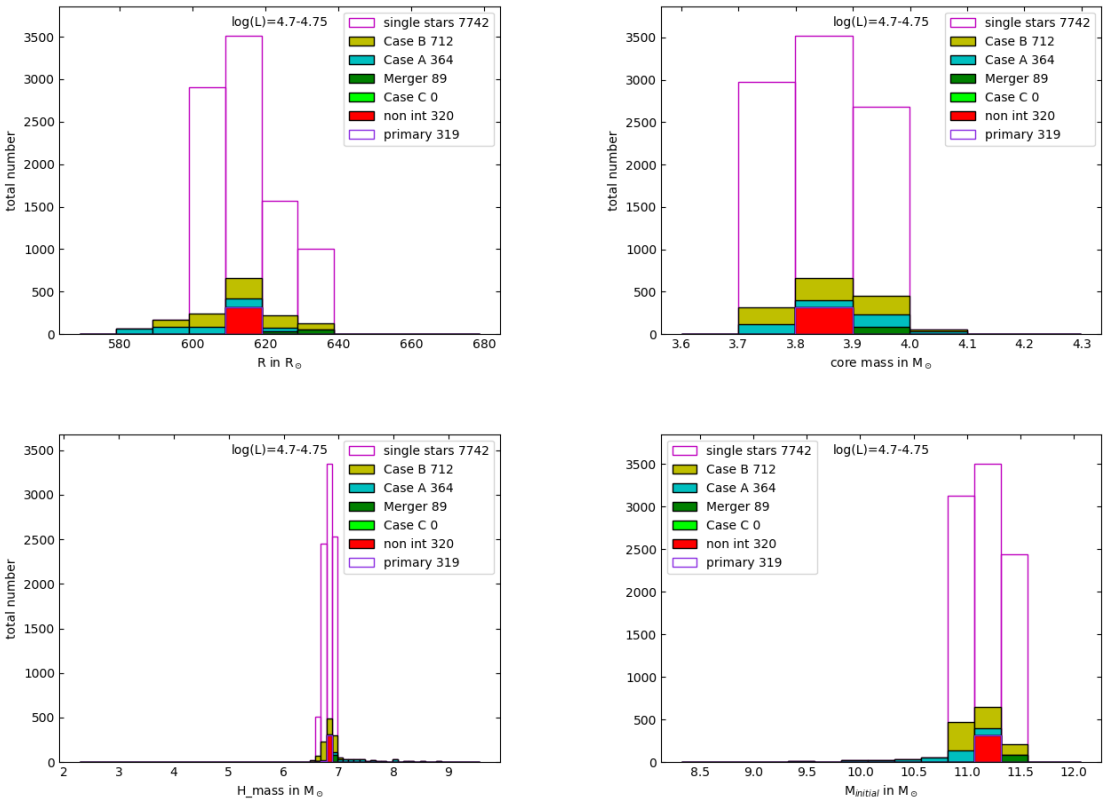

Figure A.7: Distribution of the final radius, the final core mass, the final envelope mass and the initial mass of RSGs with a final luminosity range of $log(\frac{L}{L_\odot}) = 4.7$ - 4.75

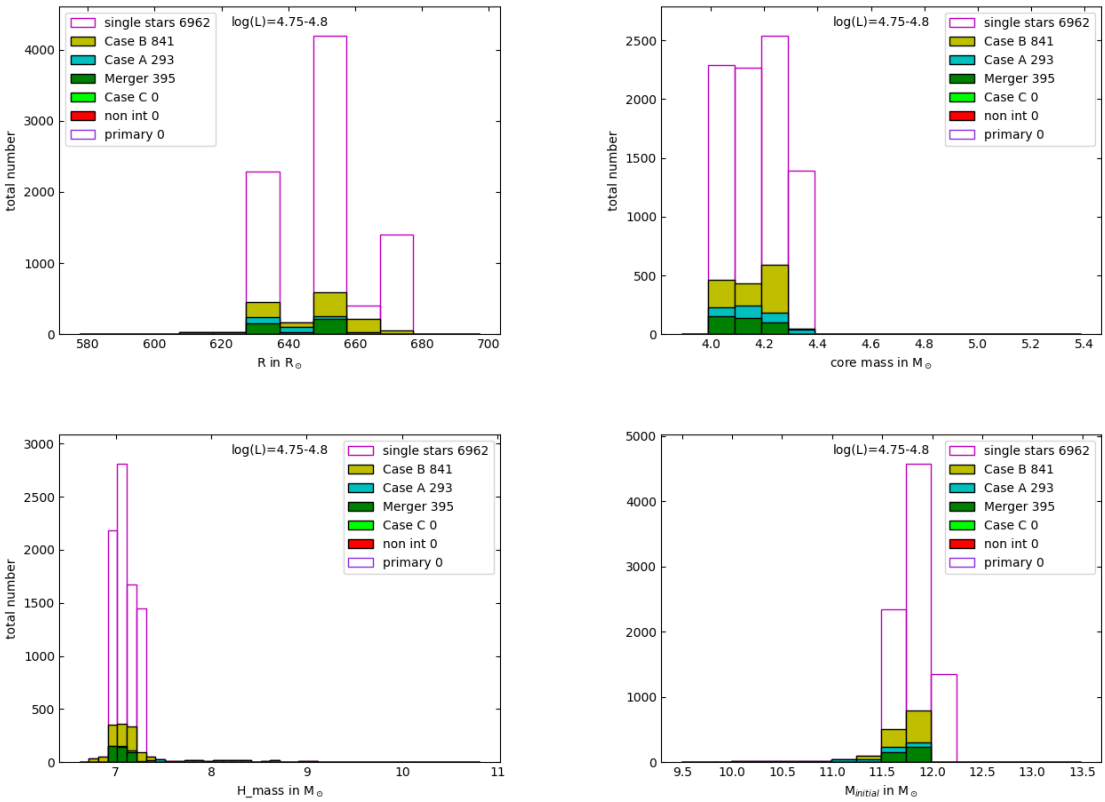

Figure A.8: As is Fig. A.7, but for a luminosity range of $log(\frac{L}{L_\odot}) = 4.75$ - 4.8

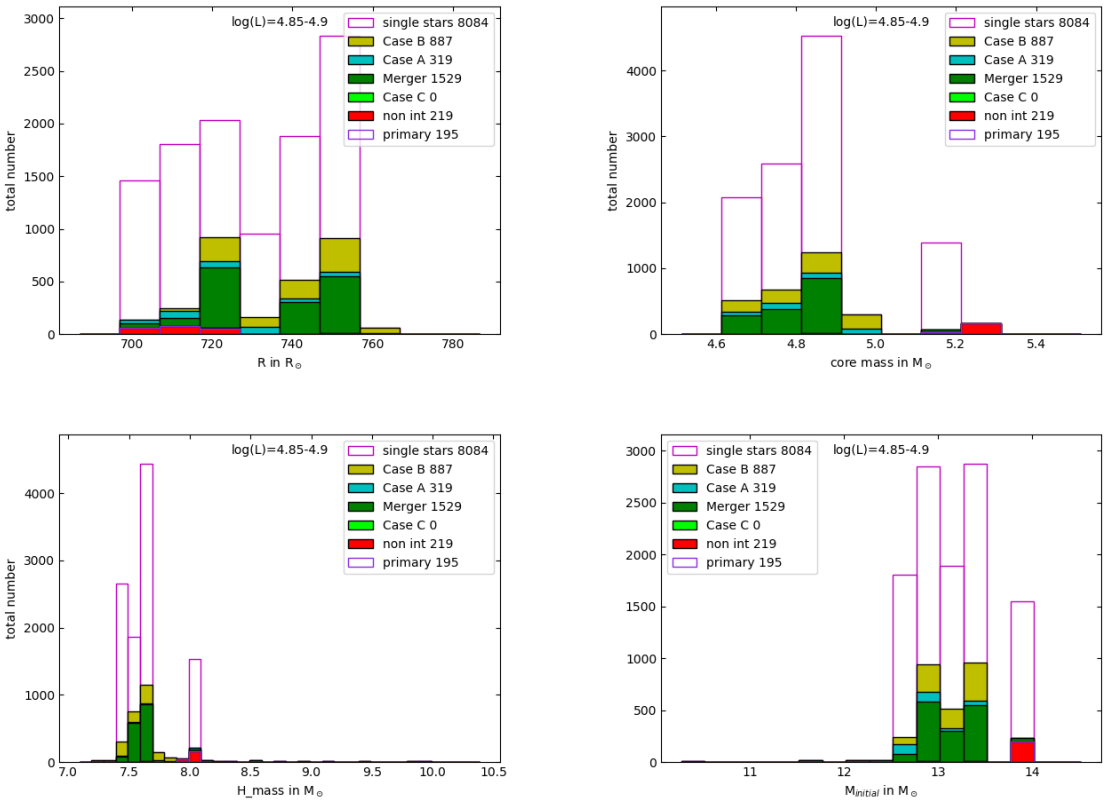

Figure A.9: As is Fig. A.7, but for a luminosity range of $log(\frac{L}{L_\odot}) = 4.85$ - 4.9

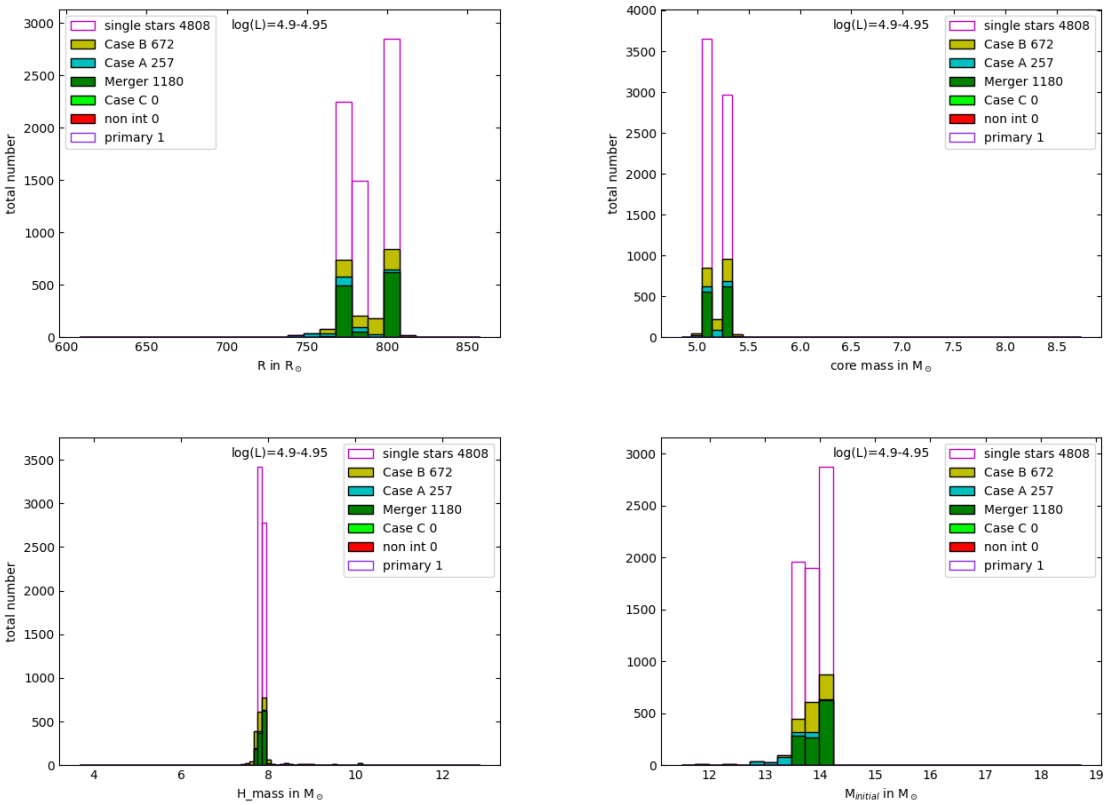

Figure A.10: As is Fig. A.7, but for a luminosity range of $log(\frac{L}{L_\odot}) = 4.9$ - 4.95

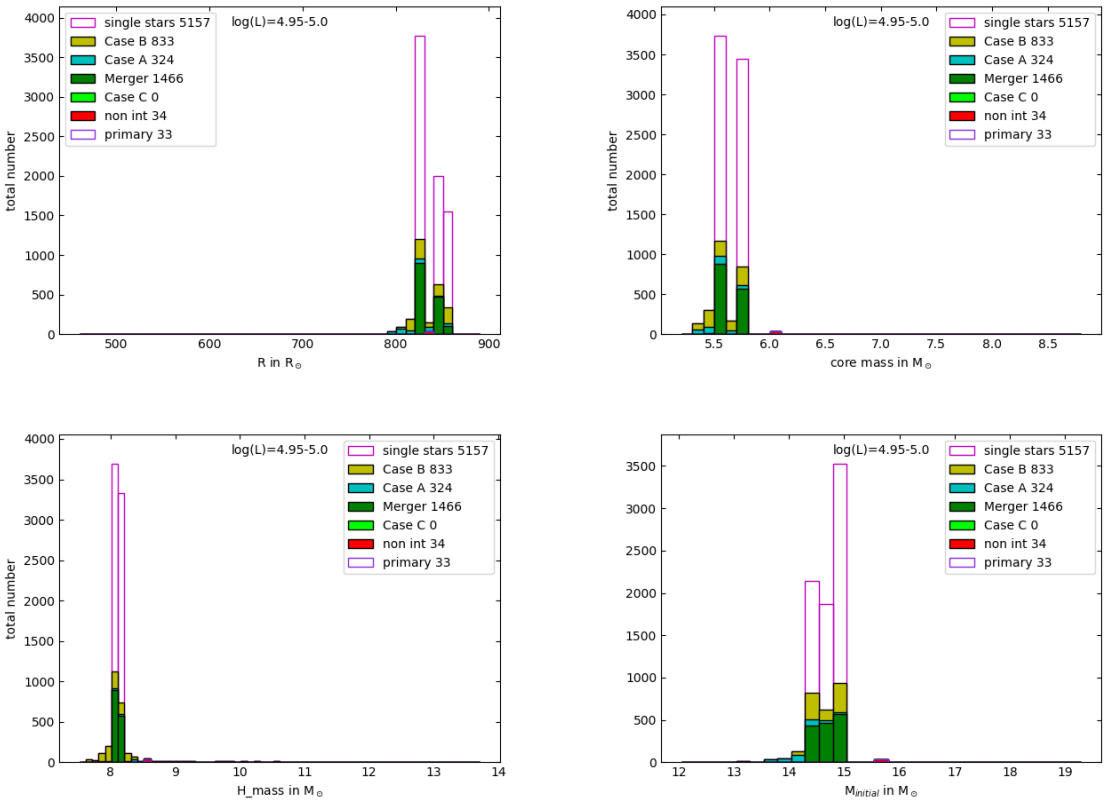

Figure A.11: As is Fig. A.7, but for a luminosity range of $log(\frac{L}{L_\odot}) = 4.95$ - 5.0

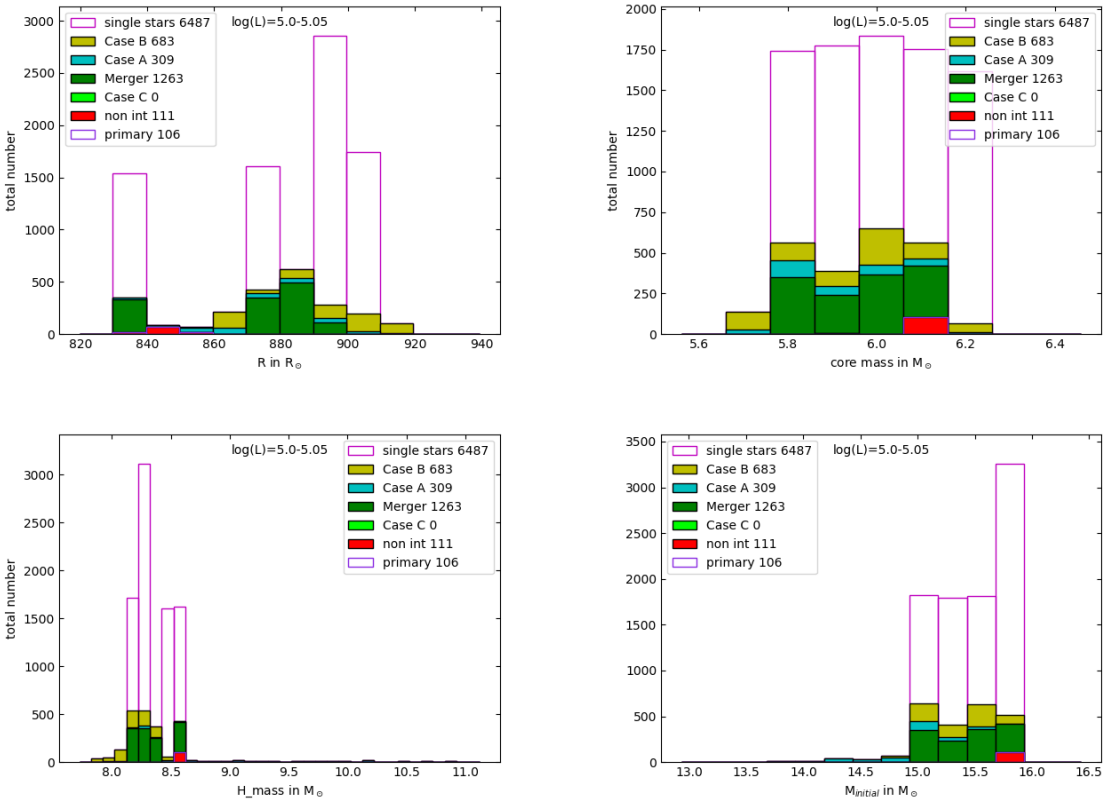

Figure A.12: As is Fig. A.7, but for a luminosity range of $log(\frac{L}{L_\odot}) = 5.0$ - 5.05

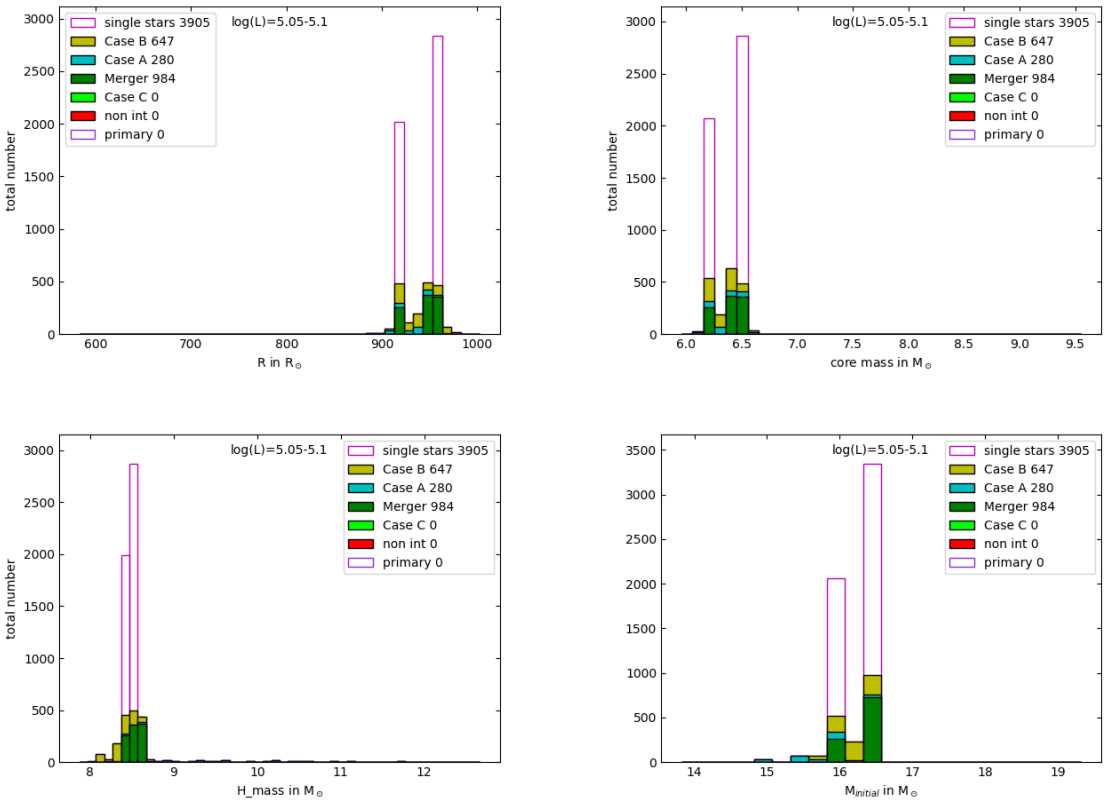

Figure A.13: As is Fig. A.7, but for a luminosity range of $log(\frac{L}{L_\odot}) = 5.05$ - 5.1